

Numerical meshing issues for three-dimensional flow simulation in journal bearings

Marcus SCHMIDT^{1*}, Peter STÜCKE¹, Matthias NOBIS²

* Corresponding author: Tel.: ++49 (0)375 5363893; Fax: ++49 (0)375 5363887;
Email: marcus.schmidt.1@fh-zwickau.de

1: Institut für Energiemanagement, Westsächsische Hochschule Zwickau, Germany

2: Forschungs- und Transferzentrum, Westsächsische Hochschule Zwickau, Germany

Abstract

Hydrodynamic journal bearings are widely used in technical and industrial applications due to their favourable wearing quality and operating characteristics. In the recent years, various experimental and numerical analyses were carried out on the design layout, the load capacity and the durability of the bearing. For typical applications the two-dimensional Reynolds differential equation is solved numerically to calculate the pressure distribution in the oil film, which is essential to simulate the dynamic behavior of the bearing. This approach however, does not allow any detailed predictions of the local three-dimensional flow structures. To understand the mechanisms, which are driven by local flow phenomena, it is necessary to solve the full Navier-Stokes-Equations in 3D together with the conservation of mass. An accurate computation of a three-dimensional flow field requires a careful discretisation of the model. Moreover, only a deliberately chosen meshing based on the optimum number of cells across the gap achieves a sufficient numerical accuracy with acceptable computational effort. This work presents variations of the mesh generation of small gaps in journal bearing models and the computed flow fields, respectively. The three-dimensional calculations are validated with measured experimental data done by Laser-Doppler-Velocimetry (LDV). In conclusion of this process the comparison of the velocity profiles of the flow field across the gap yield the necessary numerical discretisation limit applicable to the computation of the flow in journal bearings.

Keywords: Micro Flow, Journal Bearing, CFD

1. Introduction

Hydrodynamic journal bearings are widely used in technical and industrial applications due to their favorable wearing quality and operating characteristics. However, there are interactions of characteristic parameters leading to a failure of the bearing system. To detect the possible causes arising by the fluid flow, it is necessary to have knowledge of the fluid regime in the gap geometry. There are experimental and in the recent years more and more numerical methods for researching this problem. For typical applications the two-dimensional Reynolds differential equation is solved numerically to calculate the pressure distribution in the bearing gap, which is essential to simulate the dynamic behavior of the bearing. To characterize the three-

dimensional flow structures [6] it is necessary to solve the three-dimensional flow equations. Mathematically, the fluid flow is described by the Navier-Stokes equations and the conservation of mass. The solution algorithms require an optimum numerical discretisation according to numerical accuracy with acceptable computational effort.

2. Approach

2.1 Geometrical Parameters

The basic model of a journal bearing consists of two cylinders with eccentric arrangement. The stationary outer cylinder (Z2) represents the bushing of the bearing and the inner cylinder (Z1) rotates around his own middle axis with the angular speed ω_1 . The gap between the two cylinders is filled with

lubricant. A feedhole is positioned orthogonal to the outer cylinder and in the center of the bearing breadth B to supply oil into the gap. A schematic cross section of the system is shown in Fig. 1 and in equations 1 – 6 characteristic parameters are defined.

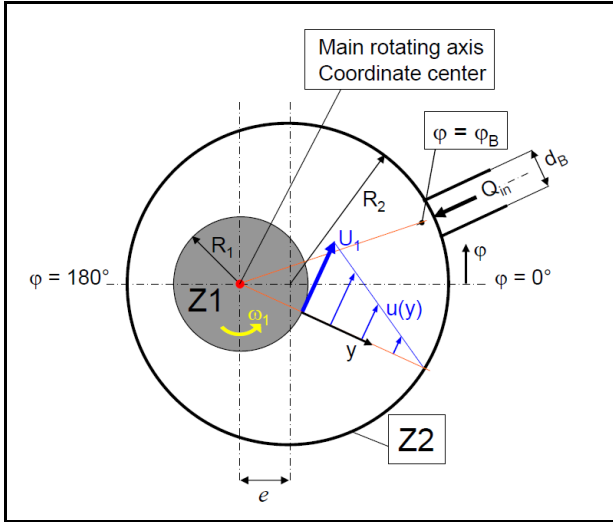


Fig. 1: cross section of the flow system

$$H_0 = R_2 - R_1 \quad (1) \quad U_1 = \omega \cdot R_1 \quad (2)$$

$$\psi = \frac{H_0}{R_1} \quad (3) \quad Re = \frac{\psi \cdot R_1 \cdot U_1}{\nu} \quad (4)$$

$$Q_0 = \frac{1}{2} \cdot B \cdot H_0 \cdot U_1 \quad (5) \quad \varepsilon = \frac{e}{R_2 - R_1} \quad (6)$$

The flow regime in journal bearings can be described by the Reynolds number. A previous study [7] classified operation ranges for journal bearings. Typical automotive applications are found in a Reynolds number range for from 10 to 40 at a clearance of $\psi = 0.1 \%$. Taking an eccentricity of $\varepsilon = 0.9$ into account, the minimum clearance shows values under $5 \mu\text{m}$. For the present paper the Reynolds number is 20 and a moderate clearance $\psi = 10 \%$ is chosen to allow flow measurements inside the oil film by means of LDV. Thus, the numerical results are validated with the experimental data.

2.2 Mathematical model

The calculations are carried out with OpenFOAM. The numerical 3D-CFD code is based on the finite-volume method and solves

the three-dimensional Navier-Stokes equations together with the continuity equation. For our project study the system is assumed to be steady, incompressible and laminar and the solved equations are reduced to equations 7 and 8. The equations are integrated on each cell (control volume) in use of the Gaussian integration. The values in the node points and face center points are approximate with linear interpolation schemes of second order. The solver uses the SIMPLE algorithm (Semi-Implicit Method for Pressure-Linked Equations) for pressure-velocity coupling.

$$(\mathbf{u} \cdot \nabla) \mathbf{u} = \frac{1}{\rho} \nabla p + \nu \nabla^2 \mathbf{u} \quad (7)$$

$$\nabla \cdot \mathbf{u} = 0 \quad (8)$$

The solution converged with successively decreasing residuals for all primitive variables below the value of 10^{-6} . The convergence rate for all solutions is 0.9 or better.

2.3 Grid generation

The grid for numerical simulation is created with the blockMesh tool included in OpenFOAM. A planar cut through the numerical grid for $\psi = 10\%$ is shown in Fig. 2. The grid generated as a block structured mesh with nearly orthogonal hexagonal cells to increase the numerical accuracy and keep the computing time acceptable. The pipe is meshed with a typical O-grid to generate wall-adapted cells for better solution quality.

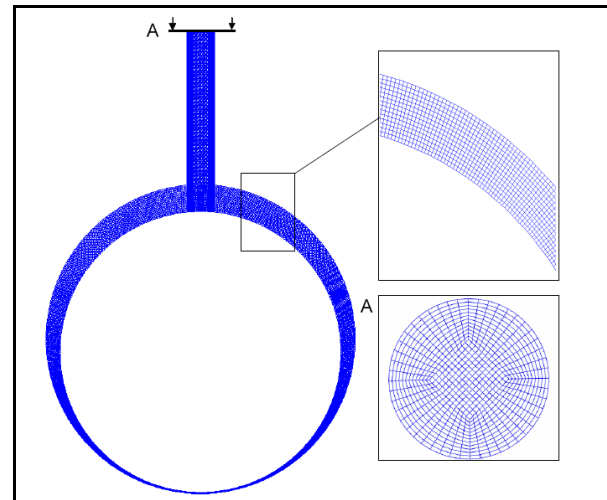


Fig. 2: computation grid for $\psi = 10\%$ and $\varepsilon = 0.9$

The position of the boundary condition at the inlet of the feedhole is modelled far away from the main solution domain to eliminate the influence of the boundary condition. The model and the boundary conditions are shown in Fig.3.

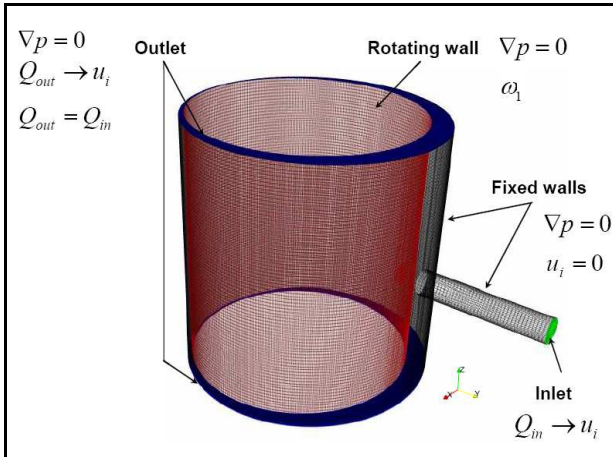


Fig. 3: boundary conditions

The inlet condition is set by a fixed velocity magnitude with a vectorial direction to characterize the incoming volumetric flow. The outlet boundaries at the both ends of the gap are modelled with a volumetric flow rate over the boundaries, so that the continuity is satisfied. The velocity of the inner rotating cylinder is defined by the rotational speed at the surface. Due to setting the pressure gradient on all boundaries to zero, there is a need to normalize the pressure in the system. Therefore, the reference pressure is introduced at the angular location of the minimum clearance or in other words, where the gap changes from convergent to divergent.

3. Results

The following results describe the validation of numerical results with experimental data obtained by LDV. With our experimental setup, displayed in Fig. 4, it is possible to measure the velocity at any circumferential position inside the oil film.

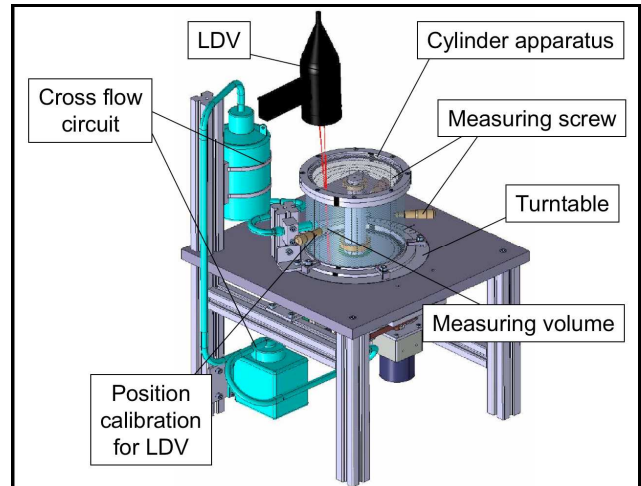


Fig. 4: experimental apparatus and LDV

For the present study, the velocity profiles adjacent to the feedhole are measured and compared at the angle of $\varphi=10.6^\circ$, which is one feedhole diameter downstream in rotation direction of the inner cylinder (Fig.5).

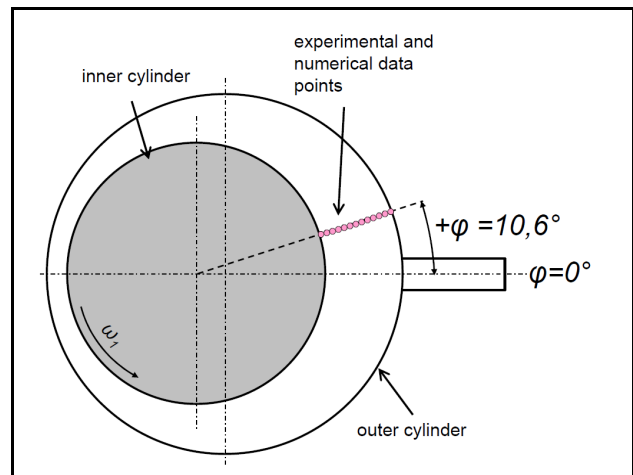


Fig. 5: experimental and numerical data points

The graphs in Fig. 6 present the distributions of normalized velocity profiles across the gap. The inner cylinder rotates with the circumferential speed U_i and the outer cylinder is at rest. The profiles are strongly affected by the incoming flow. Close to the surface of the inner cylinder, the normalized velocity is 3 times higher than the surface velocity of the rotating cylinder. In the region at the outer cylinder, a typical couette flow profile of the reversed flow is found. Hence, the overlay of incoming and Couette flow forms a fully 3D flow in the vicinity of the feedhole.

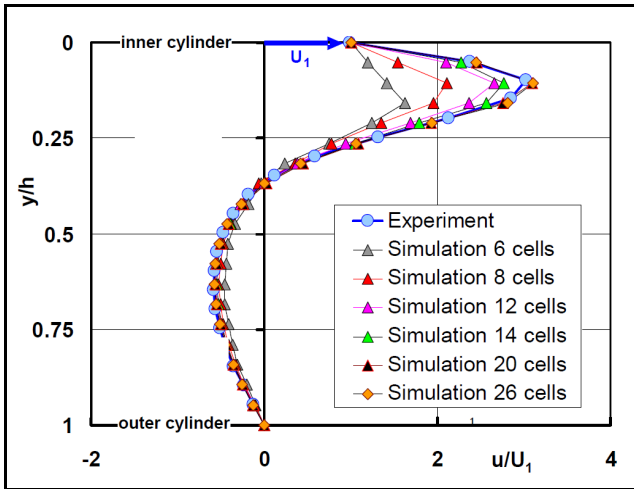


Fig. 6: Velocity profiles for $\psi = 10\%$, $\varphi_B = 0^\circ$, $Re = 20$; $\varepsilon = 90\%$

The centre of interest of the numerical study is the necessary cell number across the gap. To define the minimum of cells, which is required to simulate the flow accurately, the number of cells is increased stepwise to obtain a mesh independent solution. For a cell number of 20 across the gap the numerical solution is found to be in perfect agreement with the LDV-data. Hence, the overall cell number in the full model is one million cells. More cells would not improve the computation quality.

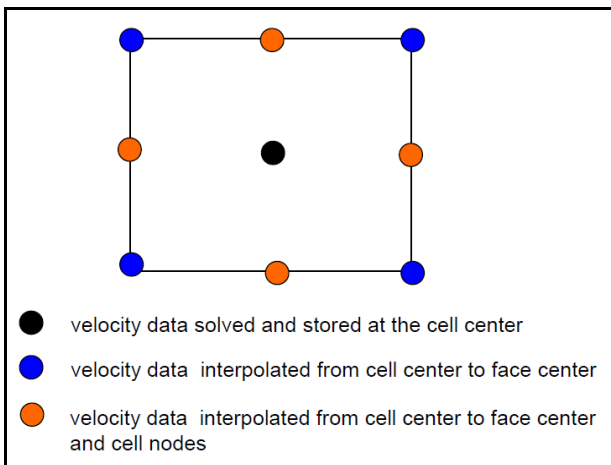


Fig. 7: schematically 2D-illustration of a grid cell

However, efforts are undertaken to reduce the total number of cells in order to minimize the computation time. One approach is the reduction of the size of the numerical model. A reduction of the required cell number of the numerical model is achieved by an improved post-processing technique.

In general, the computed results of the flow

variables are stored in the centre of the volume cells available for the post-processing process. The value density in the solution domain can be increased by means of topological interpolation between neighbor cells. Here, values of any flow variable are computed for node points and face center points, respectively. The interpolating scheme at the node and face center points is shown in Fig.7. Hence, additional supporting points for the post-processing process are available.

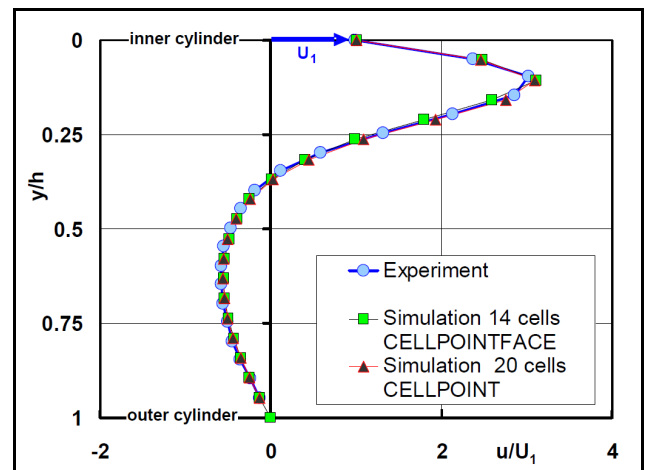


Fig. 8: Relationship of velocity profiles for $\psi = 10\%$, $\varphi_B = 0^\circ$, $Re = 20$; $\varepsilon = 90\%$

The velocity profiles, which are plotted in Fig.8, illustrate the efficiency of this approach. In comparison with the original calculation based on 20 cells across the gap, which uses only at cell centers, the result with 14 cells across the gap but additional supporting points shows the same quality in the plotted velocity profile. Hence, by means of the better post-processing process the cell number of the model can be reduced by 30 percent. Moreover, the calculation time decreases significantly.

4. Summary

The paper presents results for the required discretisation of the oil film inside hydrodynamic journal bearings for a moderate clearance. The numerical results have been validated with experimental data to prove the accuracy of the calculations. An optimized post-processing is used to decrease the numerical effort and computing capacity.

Further steps include the reduction of the normalized clearance towards smaller values in the experimental setup and in the numerical model.

The focus of the work is to determine the required number of cells with respect to the bearing clearance. Further emphasis is given to the optimization of the numerical grid, the accuracy of the calculation and the computational effort.

5. Nomenclature

| | |
|--------------------|--|
| B | breadth of the bearing |
| d_B | diameter of feedhole |
| e | eccentricity |
| h | local gap width |
| H_0 | bearing clearance |
| Q_0 | main volume flow |
| Q_{in} | volume flow of incoming oil |
| p | pressure |
| R_1 | radius of the inner cylinder |
| R_2 | radius of the outer cylinder |
| Re | Reynolds number |
| U_1 | circumferential velocity of the inner cylinder |
| $u(\varphi, y, z)$ | local circumferential fluid velocity |
| \mathbf{u} | flow velocity vector |
| φ | angle |
| ν | kinematic viscosity |
| ρ | density |
| ε | relative eccentricity |
| φ_B | angle of the feedhole position |

| | |
|------------|-------------------------------------|
| ψ | normalized clearance |
| ω_1 | angular speed of the inner cylinder |

6 References

- [1] Taylor, G.I., 1923: „Stability of a viscous liquid contained between two rotating cylinders“ Phil. Trans. Royal Soc. London.
- [2] R. C. DiPrima und H. I. Swinney 1985, Instabilities and Transition in Flow Between Two Rotating Cylinders, in Hydrodynamic Instabilities and Transition to Turbulence (Hrsg.: H. I. Swinney und J. P. Gollup), Vol. 45, Springer, New York.
- [3] Eagles, P. M., Stuart J. T., DiPrima R. C., 1978: “The Effects of Eccentricity on Torque and Load in Taylor-Vortex Flow” Journal of Fluid Mechanics, Vol. 87, pp. 209-231.
- [4] P. Stücker, M. Nobis, M. Schmidt, 2009: „3D-Flow Structures in Journal Bearings“ SAE Powertrains Fuels and Lubricants, SAE International, 2009
- [5] N. Scurtu, P. Stücker, C. Egbers, 2008: “Numerical and experimental study of the flow in an eccentric Couette-Taylor system with small gap” PAMM, Vol. 8, Issue 1, pp 10641 – 10642.
- [6] P. Stücker, M. Nobis, M. Schmidt, 2009: „Three Dimensional Flow Structures in Journal Bearings“ 2nd Micro and Nano Flows Conference, West London, UK
- [7] Nobis, M., Schmidt M., 2009: „ Experimentelle und numerische Untersuchung der Schmierspaltströmung“ Masterarbeit, Westsächsische Hochschule, Zwickau